Earth Planets Space, **59**, 133–139, 2007

In situ stress measurement by the stress relief technique using a multi-component borehole instrument

Atsushi Mukai[1], Tsuneo Yamauchi[2], Hiroshi Ishii[3], and Sigeo Matsumoto[4]

[1]*Faculty of Informatics, Nara Sangyo University, 3-12-1 Tatenokita, Sango-cho, Ikomo-gun, Nara 636-8503, Japan*
[2]*Graduate School of Environmental Studies, Nagoya University, Furo-cho, Chikusa-ku, Nagoya 464-8601, Japan*
[3]*Tono Research Institute of Earthquake Science, 1-63 Yamanouchi, Akeyo-cho, Mizunami 509-6132, Japan*
[4]*Earthquake Research Institute, University of Tokyo, 1-1-1 Yayoi, Bunkyo-ku, Tokyo 113-0032, Japan*

(Received October 26, 2004; Revised July 22, 2005; Accepted October 11, 2006; Online published March 23, 2007)

We have developed a two-dimensional method for calculating principal stresses on a plane by measuring strain changes obtained by the stress relief technique using a multi-component borehole instrument. If the ratio of the radius of the core to that of the borehole is 1.4–2.0, a uniform strain change occurs in any stress field due to the overcoring. It is therefore desirable that the radius of the core obtained by overcoring is larger than that of the borehole by a few orders of magnitude. We applied the proposed calculation method to a stress measurement performed at the Hishikari mine, southwest Japan. The maximum and minimum principal stresses were determined to be 5.0 and −0.2 MPa, respectively. The nearly vertical stress was estimated to be 1.5 MPa, which was merely 30% of the predicted vertical stress (5.6 MPa). One of causes of the small vertical stress obtained in this study is considered to be the limitation of the two-dimensional method for calculating principal stresses.

Key words: Stress relief technique, Principal stresses, multi-component borehole instrument, Two-dimensional method.

1. Introduction

The measurement of crustal stress is important for any investigation on earthquake-generating processes and the stability of underground facilities. The stress and strain in the vicinity of seismic faults and subduction zones increases during the interseismic stage (see Ruegg *et al*., 2002). Fault slips and ruptures occur when the shear stress exceeds friction along a fault. The amount of stress that occurs during an earthquake is one of the most important parameters to be considered when modeling an earthquake cycle. Underground facilities with a free surface, such as tunnels, result in the concentration of stress. It is therefore necessary to investigate the preliminarily stress field around these facilities in order to determine an effective construction process and available materials.

The primary methods for conducting in situ stress measurements are the hydraulic fracturing and stress relief techniques (e.g. Turcotte and Schubert, 1982). In general, the hydraulic fracturing technique can determine the principal stresses on a plane perpendicular to a borehole, while the stress relief technique can determine the three-dimensional state of stress. In the former, water is injected into a borehole, and the water pressure at which fractures are induced in the borehole is measured. This technique has been used for stress measurements at many sites, such as the Cajon Pass scientific research borehole (Zoback and Healy, 1992) and the KTB scientific drill holes (Brudy *et al*., 1997). In the stress relief technique, a core is obtained by overcoring at a borehole. The deformation of the core is measured using strain gauges or strainmeters (e.g. Paquin *et al*., 1982; Yokoyama, 2004): a strain gauge is attached to a hemispherical or conical base of a borehole (e.g. Sugawara and Obara, 1986; Kobayashi *et al*., 1987), while a strainmeter is installed in a borehole and attached to the surrounding crust using mortar. In the case of deep wet boreholes drilled in a soft crust, it is easier to install a strainmeter than to attach a strain gauge because strainmeters have only to be inserted along the borehole. Therefore, a strainmeter is convenient for conducting stress measurements at deep wet boreholes. However, it is more difficult to determine principal stresses using the stress relief technique with strainmeters than it is with strain gages as we cannot neglect the rigidities of the mortar and the metallic shell of the strainmeter (Sano *et al*., 2004).

In this study, we investigated the method for calculating principal stresses using strain changes obtained by the stress relief technique using a multi-component borehole instrument developed by Ishii *et al*. (2002). This instrument has displacement sensors in a thin stainless steel shell. In this measurement, the instrument is installed in a borehole filled with mortar. The mortar hardens and attaches the instrument to the surrounding crust. Due to the existence of mortar and stainless steel, the calculation of principal stresses in this measurement poses certain difficulties, as mentioned by Sano *et al*. (2004). The stress relieved by overcoring deforms the mortar and stainless steel as well as the rock in

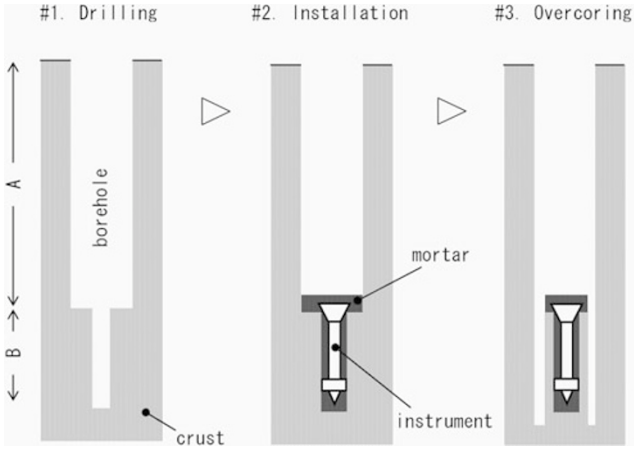

Fig. 1. Procedure for stress measurement in the stress relief technique using a multi-component borehole instrument.

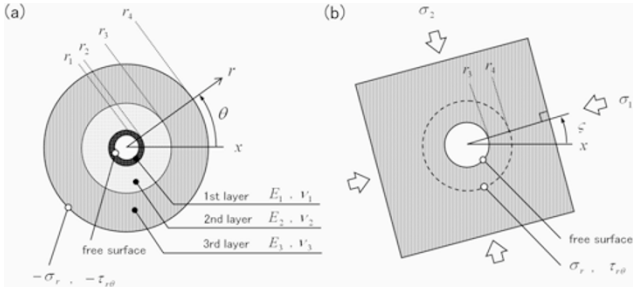

Fig. 2. Two-dimensional model of the core. (a) Cross section of the core. Radius r_4 is the outer radius of the core. r_k, E_k, and ν_k are the inner radius, Young's modulus, and Poisson's ratio of the k-th layer, respectively. (b) Radial stress σ_r and shear stress $\tau_{r\theta}$ are the stresses relieved due to overcoring, which are equivalent to the surrounding stress patterns around the borehole without mortar and the instrument. σ_1 and σ_2 are the maximum and minimum principal stresses, respectively. Angle ς is the orientation angle of σ_1.

the core. Therefore, it is necessary to consider the influence of mortar and stainless steel on the deformation of the core. The core can be approximated to a concentric cylindrical structure comprising three layers of stainless steel, mortar, and rock. Thus, we first investigated a two-dimensional analytical solution for a plane perpendicular to the borehole. Following this, we developed a calculation method of principal stresses on a plane using a core model with three layers—rock, mortar, and stainless steel. This method is valid for the following assumptions: (1) one of the principal stresses is perpendicular to the borehole; (2) the strain changes on the plane are independent of those perpendicular to it. We applied this method to the stress measurement performed at the Hishikari mine, southwest Japan.

2. Two-Dimensional Calculation Method of Principal Stresses

Figure 1 outlines the procedure for stress measurement in the stress relief technique using a multi-component borehole instrument. First, two boreholes—A and B—with a common central axis are drilled. Second, the instrument is installed in borehole B after it is filled with mortar. The mortar hardens over a period of several days and expands

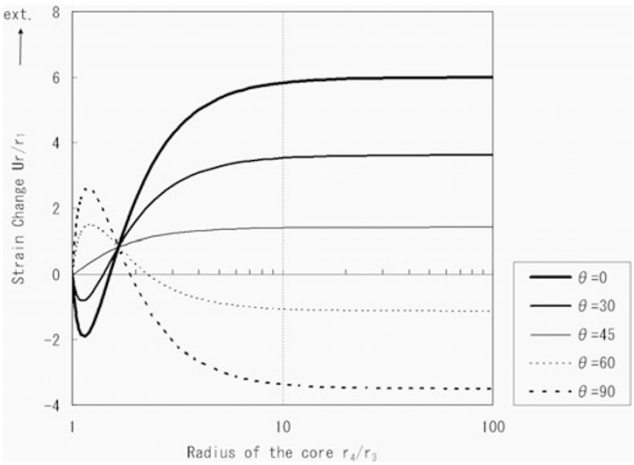

Fig. 3. Strain changes due to overcoring in the uniaxial stress field ($\sigma_1 = 1$ MPa, $\sigma_2 = 0$ MPa, $\varsigma = 0^\circ$). The axis of abscissas is the ratio of the radius of the core to that of the borehole (r_4/r_3). The strain changes were calculated from Eq. (A.27) using the values of the model parameters listed in Table 1.

Table 1. Model parameters for the calculation of principal stresses at the Hishikari mine. r_k, E_k, and ν_k are the inner radius, Young's modulus, and Poisson's ratio of the k-th layer, respectively.

	r_k [mm]	E_k [GPa]	ν_k
1st layer	16	200	0.3
2nd layer	21	20	0.2
3rd layer	30	50	0.2

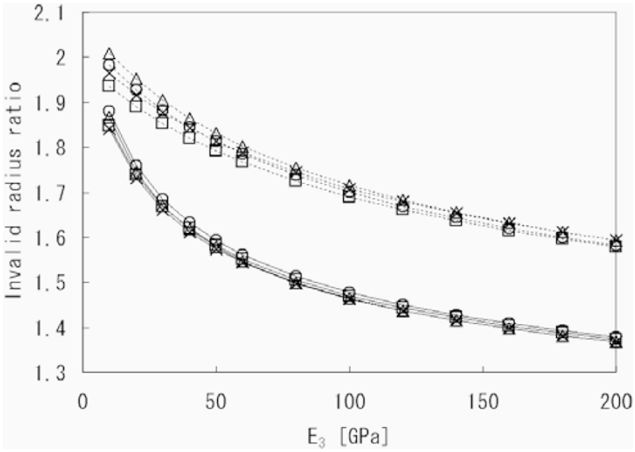

Fig. 4. Invalid radius ratio r_4/r_3, which makes stress measurement impossible. The ratio was calculated using the two-dimensional model of the core with $r_1 = 16$ mm, $r_2 = 21$ mm, $E_1 = 200$ GPa, and $\nu_1 = 0.3$. The Young's modulus of mortar (E_2) is 20 GPa (solid line) or 100 GPa (dotted line). Other model parameters are one of the following four sets: circle: $\nu_2 = \nu_3 = 0.2$, $r_3 = 31$ mm; triangle: $\nu_2 = \nu_3 = 0.2$, $r_3 = 41$ mm; square: $\nu_2 = \nu_3 = 0.4$, $r_3 = 31$ mm; and cross: $\nu_2 = \nu_3 = 0.4$, $r_3 = 41$ mm. The axis of abscissas is the Young's modulus of the rock (E_3).

by about 0.05%. Since the instrument has a battery and a memory module, it can measure strain changes for a few weeks without any external connections. Third, the overcoring is carried out and the core is cut off. The stress relieved due to overcoring causes strain changes in the core.

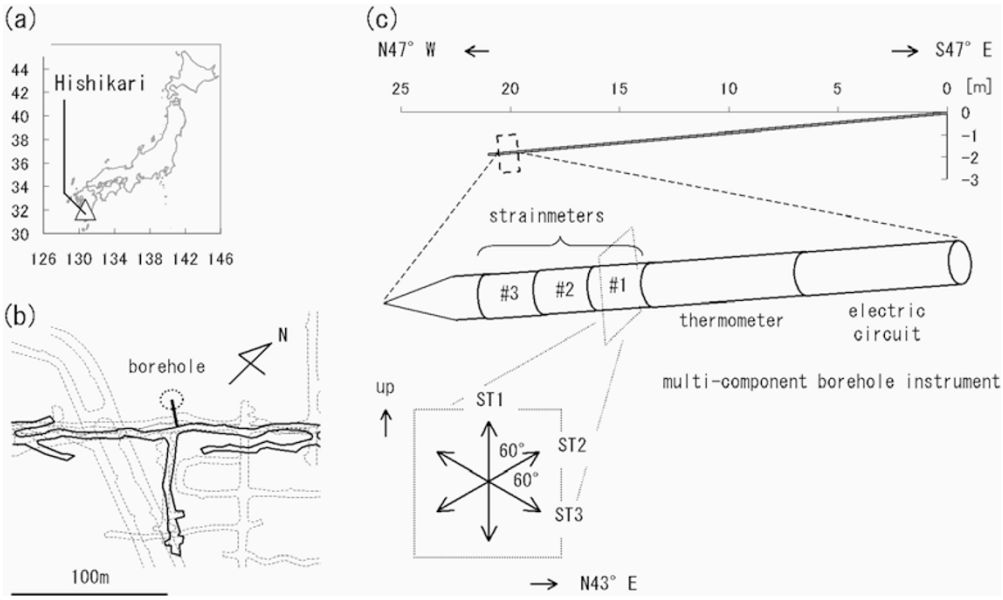

Fig. 5. Arrangements of the borehole and the multi-component borehole instrument at the Hishikari mine. (a) Location of the Hishikari mine. (b) Location of the borehole. The solid lines represent the tunnels at the depth of 220 m. A nearly horizontal borehole was drilled at this depth. The dashed lines represent the tunnels at depths of 160, 190, 250, and 280 m. (c) Arrangements of the instrument. The strainmeter modules are denoted as #1, #2, and #3. Module #1 can observe the strain changes in a direction perpendicular to the borehole. ST1, ST2, and ST3 denote strainmeters installed in module #1. Module #2 can observe the strain changes in a direction that is inclined to the borehole at 60°. Module #3 can observe the strain change along the borehole.

Subsequently, the principal stresses can be determined from the strain changes due to overcoring.

Figure 2(a) shows a cross section of the core. The core consists of three layers. The first, second, and third layers comprise stainless steel, mortar, and rock, respectively. The first layer is the outer shell of the instrument. If the expanding pressure of the mortar is ignored, the relieved stress is equivalent to the surrounding stress patterns around the borehole without the instrument and mortar (Fig. 2(b)). The radial stress σ_r and shear stress $\tau_{r\theta}$ relieved in the direction θ are expressed by the following equations (Ugural and Fenster, 2003):

$$\sigma_r = \frac{\sigma_1+\sigma_2}{2}\left(1-\frac{r_3^2}{r_4^2}\right) + \frac{\sigma_1-\sigma_2}{2}\left(1-\frac{r_3^2}{r_4^2}\right)\left(1-3\frac{r_3^2}{r_4^2}\right)\cos 2(\theta-\varsigma) \quad (1)$$

$$\tau_{r\theta} = -\frac{\sigma_1-\sigma_2}{2}\left(1-\frac{r_3^2}{r_4^2}\right)\left(1+3\frac{r_3^2}{r_4^2}\right)\sin 2(\theta-\varsigma) \quad (2)$$

where σ_1 and σ_2 are the maximum and minimum principal stresses, respectively. Angle ς is the orientation angle of the maximum principal stress. Radii r_3 and r_4 are the inner radius of the third layer and the radius of the core, respectively. Angles ς and θ are measured anticlockwise from the reference axis x, as shown in Fig. 2. Overcoring causes stress changes $-\sigma_r$ and $-\tau_{r\theta}$ on the outer surface of the core. These stress changes cause strain changes in the stainless steel and mortar as well as in the rock. The residuals of this stress remain in the core after overcoring; this is because stainless steel and mortar have no strain before overcoring and possess infinite nonzero rigidities.

In the case of a uniaxial stress field ($\sigma_1 = \sigma_0$, $\sigma_2 = 0$, $\varsigma = 0°$), the radial strain change due to overcoring is given by Eq. (A.27). Figure 3 shows the strain changes due to overcoring as a function of r_4/r_3. The strain changes in Fig. 3 were calculated using the values of the model parameters listed in Table 1 for $\sigma_1 = 1$ MPa, $\sigma_2 = 0$ MPa, and $\varsigma = 0°$. When r_4/r_3 is approximately 1.6, the strain changes due to overcoring are independent of the orientation. This implies that the principal stresses cannot be determined uniquely for $r_4/r_3 \cong 1.6$. The invalid radius ratio r_4/r_3, which makes the stress measurement impossible, depends on model parameters, such as the inner radius, Young's modulus, and Poisson's ratio of each layer. Figure 4 shows the invalid radius ratio as a function of the Young's modulus of the rock. The invalid radius ratio was calculated to be 1.4–2.0 for $r_1 = 16$ mm, $r_2 = 21$ mm, $E_1 = 200$ GPa, $\nu_1 = 0.3$, $E_2 = 20$ or 100 GPa, $\nu_2 = \nu_3 = 0.2$ or 0.4, and $r_3 = 31$ or 41 mm.

In the case of a general stress field, the radial strain changes due to overcoring are given by

$$\varepsilon(\theta) = Q_1\alpha + Q_2\beta\cos 2\theta + Q_3\beta\sin 2\theta \quad (3)$$

where $Q_1 \equiv \sigma_1+\sigma_2$, $Q_2 \equiv (\sigma_1-\sigma_2)\cos 2\varsigma$, and $Q_3 \equiv (\sigma_1-\sigma_2)\sin 2\varsigma$. Coefficients α and β are defined by Eqs. (A.28) and (A.29), respectively.

The principal stresses can be calculated by applying the least squares method to the measured strain changes $\varepsilon(\theta_1), \varepsilon(\theta_2), \ldots, \varepsilon(\theta_N)$.

$$\sigma_1 = (Q_1 + Q_2/\cos 2\varsigma)/2 \quad (4)$$

$$\sigma_2 = (Q_1 - Q_2/\cos 2\varsigma)/2 \quad (5)$$

$$\varsigma = \tan^{-1}(Q_3/Q_2)/2 \quad (6)$$

where

$$[\,Q_1 \quad Q_2 \quad Q_3\,]^T = \left(M^T M\right)^{-1} M^T$$

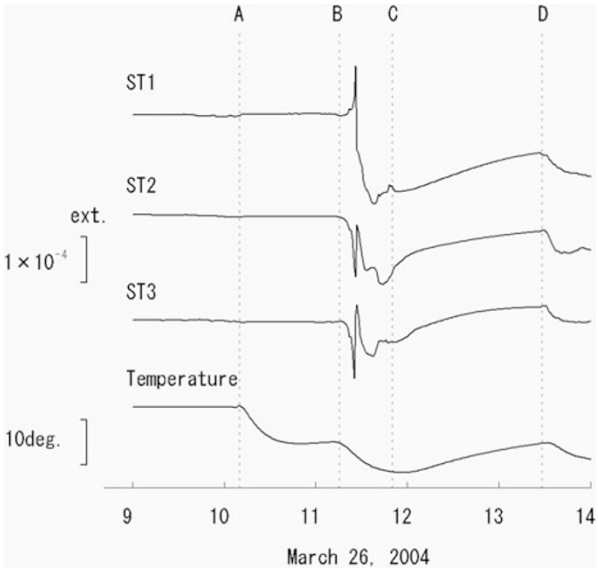

Fig. 6. Strain and temperature changes observed for 5 h on March 26, 2004. The drilling of rock adjacent to the thermometer was completed by 10:10 (A). The drilling of the rock adjacent to the strainmeters was started at 11:15 (B). Noon recess was from 11:50 (C) to 13:30 (D).

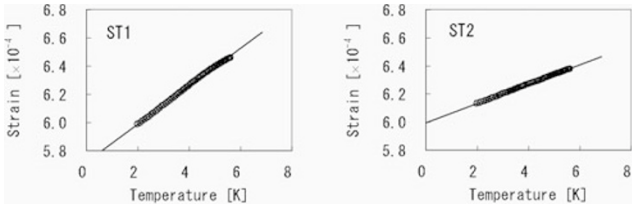

Fig. 7. Comparison between the strain changes and temperature change.

$$\times [\, \varepsilon(\theta_1) \quad \varepsilon(\theta_2) \quad \cdots \quad \varepsilon(\theta_N) \,]^T \quad (7)$$

$$M \equiv \begin{bmatrix} \alpha & \beta\cos 2\theta_1 & \beta\sin 2\theta_1 \\ \alpha & \beta\cos 2\theta_2 & \beta\sin 2\theta_2 \\ \vdots & \vdots & \vdots \\ \alpha & \beta\cos 2\theta_N & \beta\sin 2\theta_N \end{bmatrix}. \quad (8)$$

3. Stress Measurement at the Hishikari Mine

The Hishikari mine is located in Kyushu in southwest Japan (Fig. 5). Gold prospecting at this site began in 1983, and horizontal tunnels have been drilled at depths of 160, 190, 220, 250, and 280 m. The stress measurement was conducted in the tunnel at the depth of 220 m on March 26, 2004. The surrounding crust is primarily composed of andesite. The temperature in the crust is about 60°C.

As shown in Fig. 5, a 21-m-long borehole was drilled for the stress measurement. This borehole was inclined to the horizontal plane at 5° and was 131 mm in diameter between 0 and 18.7 m from inside the tunnel and 60 mm between 18.7 and 21 m. A multi-component borehole instrument was installed in the borehole (diameter: 60 mm). A core with a diameter of 102 mm was obtained by overcoring.

The multi-component borehole instrument can observe strain changes in six directions as well as temperature change. Figure 5 shows the measurement directions of three strainmeters—ST1, ST2, and ST3—which are perpendicular to the borehole. Two other strainmeters were inclined

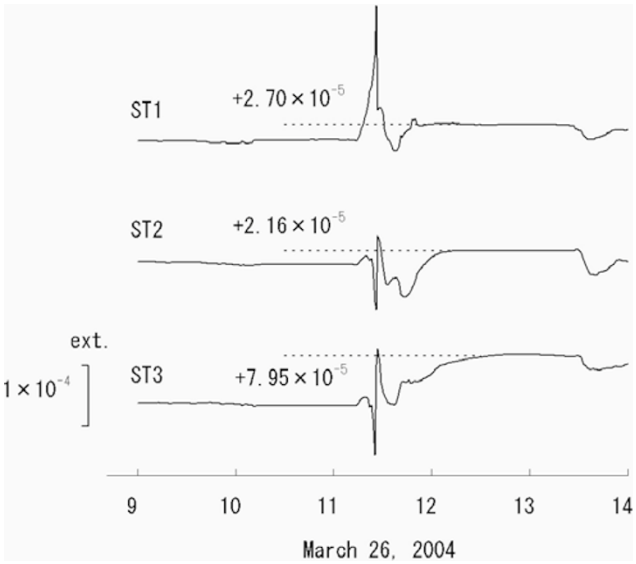

Fig. 8. Strain changes after eliminating the effect of the temperature change.

to the borehole at 60°. The sixth strainmeter observed the strain changes along the borehole. In this study, we determined the principal stresses on a plane perpendicular to the borehole by using strain changes acquired from ST1, ST2, and ST3. The strike of the nearly vertical plane is in the northeast- southwest direction.

Figure 6 shows the strain and temperature changes observed at intervals of every 1 min for 5 h before and after the overcoring. The recorded resolutions of the strain and temperature changes were about 3×10^{-12} and 1×10^{-3}°C, respectively.

4. Analysis

At approximately 10:10 on March 26, 2004, the rock adjacent to the thermometer of the instrument was drilled during the overcoring at the Hishikari mine. Water was injected into the borehole during the overcoring to reduce frictional heat. The temperature of the water was about 40°C, while the temperature of the crust was about 60°C. The injected water reduced the temperature of the core by 8°C (Fig. 6). Rapid strain changes occurred immediately after 11:15, when the rock adjacent to the strainmeters was drilled. Strain compressions resulted from the rapid cooling that occurred following the injection of the water.

Overcoring was temporarily suspended during the noon recess from 11:50 to 13:30, during which time the core was allowed to remain in the crust. As shown in Fig. 6, strain extension and an increase in temperature were observed during the recess as a result of the warming and subsequent expansion of the core due to the heat of the crust. Figure 7 shows the comparison between the strain changes and temperature change during the latter half of the recess. The strain changes at ST1, ST2, and ST3 were proportional to the temperature change with proportionality factors of 13.5×10^{-5}, 6.9×10^{-5}, and 5.8×10^{-5} K^{-1}, respectively. These factors were of the same order as that of the linear expansion coefficients of andesite, mortar, and stainless steel (10^{-5} K^{-1}).

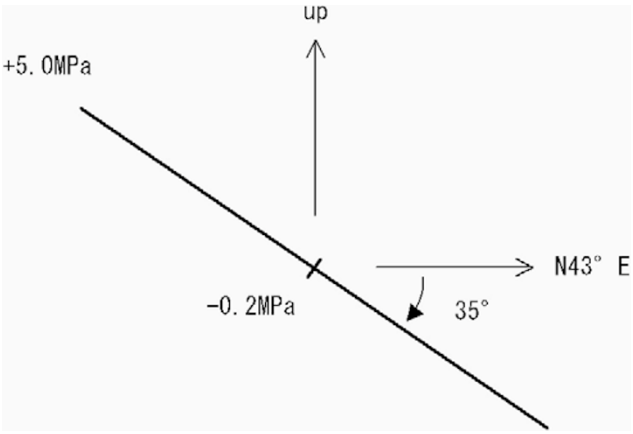

Fig. 9. Determined principal stresses. Positive stress indicates compression. The "up" direction is inclined to the vertical at 5°.

Figure 8 shows the strain changes obtained after eliminating the effect of the temperature change. Strain changes at ST1, ST2, and ST3 due to overcoring indicated extensions of 2.7×10^{-5}, 2.2×10^{-5} and 8.0×10^{-5}, respectively. Principal stresses were estimated by applying the calculation method described in Section 2 to the strain changes due to overcoring. Table 1 lists the values of the model parameters used for the calculation. The Young's modulus and Poisson's ratio of the rock listed in Table 1 are the averaged elastic constants of andesite (Lama and Vutukuri, 1978). Figure 9 shows the determined principal stresses. The maximum and minimum principal stresses were 5.0 ± 0.1 MPa and -0.2 ± 0.1 MPa, respectively. The dip angle of the maximum principal stress was $35 \pm 1°$.

5. Discussion

When the stress measurement is carried out by the stress relief technique using a multi-component borehole instrument, the core obtained by overcoring has three layers - rock, mortar, and stainless steel. We must consider the influences of the mortar and stainless steel on the strain changes due to the relieved stress in order to determine the principal stresses. If the core has only a rock layer, or if the Young's moduli of the mortar and stainless steel are negligibly small, the strain changes due to overcoring are independent of the core radius. However, the practical strain changes due to overcoring depend on the core radius because the relieved stress deforms the mortar and stainless steel, which have infinite nonzero rigidities, as well as the rock.

When the strain changes due to overcoring are calculated for the values of the model parameters listed in Table 1, it is observed that they are independent of the orientation when the ratio of the radius of the core to that of the borehole (r_4/r_3) is about 1.6 (Fig. 3). In this case, we cannot determine the principal stresses uniquely. The radius ratio r_4/r_3 was 1.7 for the overcoring at the Hishikari mine; consequently, we were thus able to determine the principal stresses. The invalid radius ratio r_4/r_3, which makes the stress measurement impossible, was calculated to be 1.4–2.0 for $r_1 = 16$ mm, $r_2 = 21$ mm, $E_1 = 200$ GPa, $\nu_1 = 0.3$, $E_2 = 20$ or 100 GPa, $\nu_2 = \nu_3 = 0.2$ or 0.4, and $r_3 = 31$ or 41 mm (Fig. 4). This result suggests that with respect to the overcoring, it is desirable that the radius of the core be larger than that of the borehole by a few orders of magnitude.

The stress measurement at the Hishikari mine was performed at the depth of 220 m. If the density of the crust is 2.5 g/cm^3, then the vertical stress is predicted to be approximately 5.6 MPa. We determined that at the Hishakari mine, the principal stresses on the plane were inclined to the vertical at 5°. By using the principal stresses shown in Fig. 9, the nearly vertical stress was estimated to be 1.5 MPa; this was merely 30% of the predicted vertical stress. In this study, we used the two-dimensional analytical solution for a plane perpendicular to the borehole. This solution is valid for the following assumptions: (1) one of the principal stresses is proportional to the borehole; (2) the strain changes on the plane are independent of those perpendicular to it. However, these assumptions are not adequate for the general crust. If an isotropic homogeneous crust with a Poisson's ratio of 0.2 is subjected to uniform stresses, the principal stress on a plane estimated under these assumptions would have an error of 25%. We propose that the small vertical stress obtained in this study is due to the limitation of the two-dimensional model. In future studies, we should investigate a three-dimensional solution for the stress relief technique for a more precise analysis.

6. Conclusions

We developed a two-dimensional calculation method of principal stresses on a plane by measuring strain changes obtained by the stress relief technique using a multi-component borehole instrument. The cross section of a core obtained by overcoring can be approximated to be a two-dimensional model comprising three layers—stainless steel, mortar, and rock. Strain residuals remain in the core after overcoring because the relieved stress deforms the stainless and mortar as well as the rock of the core. If the ratio of the radius of the core to that of the borehole is 1.4–2.0, uniform strain change occurs by overcoring carried out in any stress field. Thus, it is desirable that the radius of the core is larger than that of the borehole by a few orders of magnitude. We applied the proposed calculation method to the stress measurement performed at the Hishikari mine, southwest Japan. Principal stresses were calculated on a plane that was inclined to the vertical at 5°. The maximum and minimum principal stresses were determined to be 5.0 MPa and −0.2 MPa, respectively. The nearly vertical stress was estimated to be 1.5 MPa and was merely 30% of the predicted vertical stress (5.6 MPa). The proposed two-dimensional calculation method is valid for the following assumptions: (1) one of the principal stresses is proportional to the borehole; (2) the strain changes on the plane are independent of those perpendicular to it. In the case of an isotropic homogeneous crust with a Poisson's ratio of 0.2 under a uniform stress field, any neglect of the effect of the perpendicular stress reduces the estimated stress on a plane by 25%. One of causes of the small vertical stress obtained in this study is considered to be the limitation of the two-dimensional calculation method.

Appendix. Strain changes due to overcoring under uniaxial compression

As shown in Fig. 2, a core obtained by overcoring can be approximated to a concentric cylindrical structure comprising three layers—stainless steel, mortar, and rock. We first consider the plane strain problem for a homogeneous isotropic elastic annulus and obtain an analytical solution for the deformation of one annulus layer subjected to internal and external stresses. Second, we obtain an analytical solution for the deformation of three concentric annulus layers that are subjected to the stress relieved as a result of the overcoring.

(a) Deformation of an annulus subjected to internal and external stresses

An annulus with an inner radius a and b outer radius is subjected to the following radial (σ_r) and shear ($\tau_{r\theta}$) stresses:

$$\sigma_r = q_{11} + q_{12}\cos 2\theta \quad \text{at} \quad r = a \tag{A.1}$$
$$\tau_{r\theta} = q_{13}\sin 2\theta \quad \text{at} \quad r = a \tag{A.2}$$
$$\sigma_r = q_{21} + q_{22}\cos 2\theta \quad \text{at} \quad r = b \tag{A.3}$$
$$\tau_{r\theta} = q_{23}\sin 2\theta \quad \text{at} \quad r = b \tag{A.4}$$

where r and θ are the radial distance and angle, respectively.

A part of the two-dimensional problems in elastic deformations can be analytically solved using Airy's stress function and boundary conditions on stress (e.g. Nakahara, 1977). The stresses (A.1)–(A.4) cause the following radial (u_r) and azimuthal (u_θ) displacements in the annulus:

$$\frac{u_r}{r} = \sum_{k=1}^{2}\left\{ A_k\,(r, E, \nu, a, b)\, q_{k1} + \sum_{j=2}^{3} B_{kj}\,(r, E, \nu, a, b)\, q_{kj}\cos 2\theta \right\} \tag{A.5}$$
$$\frac{u_\theta}{r} = \sum_{k=1}^{2}\sum_{j=2}^{3} C_{kj}\,(r, E, \nu, a, b)\, q_{kj}\sin 2\theta \tag{A.6}$$

where

$$A_k \equiv \frac{1}{E}\begin{bmatrix} 2(1-\nu) \\ -(1+\nu)\,r^{-2} \end{bmatrix}^T \begin{bmatrix} 2 & a^{-2} \\ 2 & b^{-2} \end{bmatrix}^{-1} \begin{bmatrix} \delta_{k1} \\ \delta_{k2} \end{bmatrix} \tag{A.7}$$

$$B_{kj} \equiv \frac{1}{E}\begin{bmatrix} -4\nu r^2 \\ -2(1+\nu) \\ 4r^{-2} \\ 2(1+\nu)\,r^{-4} \end{bmatrix}^T N^{-1} \begin{bmatrix} \delta_{k1}\delta_{j2} \\ \delta_{k1}\delta_{j3} \\ \delta_{k2}\delta_{j2} \\ \delta_{k2}\delta_{j3} \end{bmatrix} \tag{A.8}$$

$$C_{kj} \equiv \frac{1}{E}\begin{bmatrix} 2(3+\nu)\,r^2 \\ 2(1+\nu) \\ -2(1-\nu)\,r^{-2} \\ 2(1+\nu)\,r^{-4} \end{bmatrix}^T N^{-1} \begin{bmatrix} \delta_{k1}\delta_{j2} \\ \delta_{k1}\delta_{j3} \\ \delta_{k2}\delta_{j2} \\ \delta_{k2}\delta_{j3} \end{bmatrix} \tag{A.9}$$

$$N \equiv \begin{bmatrix} 0 & -2 & -4a^{-2} & -6a^{-4} \\ 6a^2 & 2 & -2a^{-2} & -6a^{-4} \\ 0 & -2 & -4b^{-2} & -6b^{-4} \\ 6b^2 & 2 & -2b^{-2} & -6b^{-4} \end{bmatrix} \tag{A.10}$$

E, ν, and δ_{ij} indicate the Young's modulus, Poisson's ratio and Kronecker's delta, respectively.

(b) Deformation of the three annulus layers subjected to the stress relieved due to overcoring

We investigate the deformation of the core with three annulus layers shown in Fig. 2 by using Eqs. (A.5)–(A.10) for the abovementioned deformation of an annulus. If the overcoring is carried out in the stress field of uniaxial compression σ_0 in the direction $\theta = 0$, then the radial and shear stresses relieved on the outside of the core are

$$\sigma_r = \sigma_0\,(p_{31} + p_{32}\cos 2\theta) \tag{A.11}$$
$$\tau_{r\theta} = \sigma_0 p_{33}\sin 2\theta \tag{A.12}$$

where

$$p_{31} \equiv 1 - r_3^2/r_4^2 \tag{A.13}$$
$$p_{32} \equiv \left(1 - r_3^2/r_4^2\right)\left(1 - 3r_3^2/r_4^2\right) \tag{A.14}$$
$$p_{33} \equiv \left(1 - r_3^2/r_4^2\right)\left(1 + 3r_3^2/r_4^2\right) \tag{A.15}$$

where r_3 and r_4 are the radii of the borehole and the core, respectively.

The overcoring causes the following stress changes on the boundaries:

$$\sigma_r = \sigma_0\,(p_{11} + p_{12}\cos 2\theta) \quad \text{at} \quad r = r_2 \tag{A.16}$$
$$\tau_{r\theta} = \sigma_0 p_{13}\sin 2\theta \quad \text{at} \quad r = r_2 \tag{A.17}$$
$$\sigma_r = \sigma_0\,(p_{21} + p_{22}\cos 2\theta) \quad \text{at} \quad r = r_3 \tag{A.18}$$
$$\tau_{r\theta} = \sigma_0 p_{23}\sin 2\theta \quad \text{at} \quad r = r_3. \tag{A.19}$$

The inner surface of the stainless layer is a free surface and the stress changes at $r = r_1$ are zero.

The continuity of displacement on the boundary yields the following six equations that are derived from Eqs. (A.5) and (A.6):

$$A_2\,(r_2, E_1, \nu_1, r_1, r_2)\, p_{11} = \sum_{k=1}^{2} A_k\,(r_2, E_2, \nu_2, r_2, r_3)\, p_{k1} \tag{A.20}$$

$$\sum_{j=2}^{3} B_{2j}\,(r_2, E_1, \nu_1, r_1, r_2)\, p_{2j} = \sum_{k=1}^{2}\sum_{j=2}^{3} B_{kj}\,(r_2, E_2, \nu_2, r_2, r_3)\, p_{kj} \tag{A.21}$$

$$\sum_{j=2}^{3} C_{2j}\,(r_2, E_1, \nu_1, r_1, r_2)\, p_{2j} = \sum_{k=1}^{2}\sum_{j=2}^{3} C_{kj}\,(r_2, E_2, \nu_2, r_2, r_3)\, p_{kj} \tag{A.22}$$

$$\sum_{k=1}^{2} A_k\,(r_3, E_2, \nu_2, r_2, r_3)\, p_{k1} = \sum_{k=1}^{2} A_k\,(r_3, E_3, \nu_3, r_3, r_4)\, p_{(k+1)1} \tag{A.23}$$

$$\sum_{k=1}^{2}\sum_{j=2}^{3} B_{kj}\,(r_3, E_2, \nu_2, r_2, r_3)\, p_{kj} = \sum_{k=1}^{2}\sum_{j=2}^{3} B_{kj}\,(r_3, E_3, \nu_3, r_3, r_4)\, p_{(k+1)j} \tag{A.24}$$

$$\sum_{k=1}^{2}\sum_{j=2}^{3} C_{kj}\,(r_3, E_2, \nu_2, r_2, r_3)\, p_{kj}$$

$$= \sum_{k=1}^{2} \sum_{j=2}^{3} C_{kj}\,(r_3, E_3, \nu_3, r_3, r_4)\; p_{(k+1)j}. \quad \text{(A.25)}$$

We can solve p_{11}, p_{12}, and p_{13} using Eqs. (A.20)–(A.25) since p_{31}, p_{32}, and p_{33} are known.

$$p_{1j} = f_j\,(p_{31}, p_{32}, p_{33}) \qquad (j = 1, 2, 3). \quad \text{(A.26)}$$

Finally, the radial displacement on the inner surface of the stainless layer can be calculated as follows:

$$\left.\frac{u_r}{r}\right|_{r=a} = \sigma_0\,(\alpha + \beta \cos 2\theta) \quad \text{(A.27)}$$

where

$$\alpha \equiv A_2\,(r_1, E_1, \nu_1, r_1, r_2)\; f_1 \quad \text{(A.28)}$$

$$\beta \equiv B_{22}\,(r_1, E_1, \nu_1, r_1, r_2)\; f_2 + B_{23}\,(r_1, E_1, \nu_1, r_1, r_2)\; f_3. \quad \text{(A.29)}$$

References

Brudy, M., M. D. Zoback, K. Fuchs, F. Rummel, and J. Baumgartner, Estimation of the complete stress tensor to 8 km depth in the KTB scientific drill holes: Implications for crustal strength, *J. Geophys. Res.*, **102**, 18453–18475, 1997.

Ishii, H., T. Yamauchi, S. Matsumoto, Y. Hirata, and S. Nakao, Development of multi-component borehole instrument for earthquake prediction study: some observed examples of precursory and co-seismic phenomena relating to earthquake swarms and application of the instrument for rock mechanics, in *Seismogenic Process Monitoring*, 365–377, Balkema, Rotterdam, 2002.

Kobayashi, S., N. Nishimura, and K. Matsumoto, Displacements and strains around a non-flat-end borehole, Proc. 2nd Int. Symp. Field Measurements Geomech., Kobe, 2, 1079–1084, 1987.

Lama, R. D. and V. S. Vutukuri, Handbook on mechanical properties of rocks—testing techniques and results, Volume II, Trans Tech Publications, 1978.

Nakahara, I., *Applied Elasticity*, Jikkyo Publications, 1977 (in Japanese).

Paquin, C., C. Froidevaux, J. Blyet, Y. Ricard, and C. Angelidis, Tectonic stresses on the mainland of Greece: in situ measurements by overcoring, *Tectonophysics*, **86**, 17–26, 1982.

Ruegg, J. C., J. Campos, R. Madariaga, E. Kausel, J. B. de Chabalier, R. Amijo, D. Dimitrov, I. Georgiev, and S. Barrientos, Interseismic strain accumulation in south central Chile from GPS measurements, 1996–1999, *Geophys. Res. Lett.*, **29**, doi: 10.1029/2001GL013438, 2002.

Sano, O., H. Itou, and Y. Mizuta, A consideration for precise measurement of the crustal stress, *Monthly Chikyu*, **26**, 39–55, 2004 (in Japanese).

Sugawara, K. and Y. Obara, Measurement of in-situ rock stress by hemispherical-ended borehole technique, *Int. J. Min. Sci. Tech.*, **3**, 287–300, 1986.

Turcotte, D. L. and G. Schubert, *Geodynamics Applications of Continuum Physics to Geological Problems*, John Wiley & Sons, Inc., 1982.

Ugural, A. C. and S. K. Fenster, Advanced strength and applied elasticity, Prentice Hall Professional Technical Reference., 2003.

Yokoyama, T., The state of the stress relief methods and the assignments, *Monthly Chikyu*, **26**, 13–19, 2004 (in Japanese).

Zoback, M. D. and J. H. Healy, In situ stress measurement to 3.5 km depth in the Cajon Pass Scientific Research Borehole: Implications for the mechanics of crustal faulting, *J. Geophys. Res.*, **97**, 5039–5057, 1992.

A. Mukai (e-mail: mukai-landy@sage.ocn.ne.jp), T. Yamauchi, H. Ishii, and S. Matsumoto